



Mechanical properties of the ferroelectric metal-free perovskite [MDABCO](NH₄)I₃†

Cite this: *Chem. Commun.*, 2019, 55, 3911

Received 22nd January 2019,
Accepted 4th March 2019

DOI: 10.1039/c9cc00580c

rsc.li/chemcomm

Michael G. Ehrenreich,^a Zhixin Zeng,^{id}^b Stefan Burger,^{id}^a Mark R. Warren,^c
Michael W. Gaultois,^{id}^d Jin-Chong Tan^{id}*^b and Gregor Kieslich^{id}*^a

The metal-free hybrid organic–inorganic perovskite [MDABCO](NH₄)I₃ (with MDABCO = *N*-methyl-1,4-diazabicyclo[2.2.2]octane) was recently discovered to exhibit an excellent ferroelectric performance, challenging established ceramic ferroelectrics. We here probe the mechanical properties of [MDABCO](NH₄)I₃ by combining high pressure single crystal X-ray diffraction and nanoindentation, underlining the exceptional role and opportunities that come with the use of sustainable, metal-free perovskite ferroelectrics.

ABX₃ hybrid organic–inorganic perovskites (HOIPs) combine many fundamental and application-oriented properties in one materials family, providing a fascinating platform for studying structure–property relations across different aspects of materials science.¹ Like their all-inorganic parents, HOIPs adopt a 3D perovskite-motif where the B-cation and X-anion form a ReO₃-type network and the A-site cation is located in the void of this network. In contrast to all-inorganic perovskites, however, either the A, B or X ion is a molecular building unit, making the material a hybrid. Prototypical HOIPs are [CH₃NH₃]PbI₃ and [(NH₂)₂CH]PbI₃, which recently led to a change in paradigm for high-efficiency photovoltaic devices.^{2,3} Likewise, HOIPs such as [(CH₃)₂NH₂]Mn(HCOO)₃ and [TPrA]Mn(dca)₃ (with TPrA = tetrapropylammonium and dca = dicyanamide) exhibit multiferroic properties and offer fascinating opportunities as next-generation working media in mechanocalorics.^{4,5}

Whilst the general structure-motif and building-principle of HOIPs and all-inorganic perovskites is similar, *i.e.* the Goldschmidt's Tolerance Factor concept is applicable to both families with only a few exceptions,^{6,7} the possibility to introduce molecular ions offers additional opportunities such as weak molecular interactions that can be used for materials design.^{8,9} For instance, it was shown that hydrogen bonding interactions between the A-cation and the negatively charged ReO₃-type framework in HOIPs such as [CH₃NH₃]PbI₃ or [NH₃NH₂]Zn(HCOO)₃ play an important role in the order-disorder phase transitions as a function of temperature.^{10,11} Such interactions are intrinsically absent in all-inorganic perovskites and provide an important toolkit for manipulating physical properties through crystal chemistry approaches, such as the introduction of symmetry-breaking phenomena and functional groups.^{12–14}

The additional control provided by molecular components has already enabled a symmetry-based molecular design strategy that has led to the synthesis and subsequent discovery of striking ferroelectric performance in the HOIP [MDABCO](NH₄)I₃.¹⁵ For instance, choosing [MDABCO]²⁺ as a divalent A-site cation with C_{3v} point-symmetry permits the formation of a HOIP that exhibits a noncentrosymmetric space-group and unique crystallographic axis. These parameters are prerequisites for ferroelectricity in crystalline materials such as Rochelle salt,¹⁶ BaTiO₃, Pb(Zr_{1-x}Ti_x)O₃ or [(CH₃)₂CH]₂NH₂Br.¹⁷ Comparing the ferroelectric performance of [MDABCO](NH₄)I₃ to state-of-the-art ceramic ferroelectrics such as BaTiO₃ and Pb(Zr_{1-x}Ti_x)O₃,¹⁸ [MDABCO](NH₄)I₃ exhibits a similarly large spontaneous polarization (22 μC cm⁻²).¹⁵ In contrast to established ferroelectric ceramics, [MDABCO](NH₄)I₃ is synthesized at room temperature based on a slow-diffusion approach,^{15,19} immediately raising the opportunity of large scale synthesis processes and easy drop-cast or spin coating preparation techniques for thin film ferroelectric devices. Together with the absence of any heavy metals that might raise health and environmental concerns, [MDABCO](NH₄)I₃ seems to have the potential to spark a new era of metal-free high performance ferroelectric materials. One key issue for future

^a Department of Chemistry and Catalysis Research Center, Technical University of Munich, Lichtenbergstrasse 4, D-85748 Garching, Germany. E-mail: gregor.kieslich@tum.de

^b Multifunctional Materials & Composites (MMC) Laboratory, Department of Engineering Science, University of Oxford, Oxford OX1 3PJ, UK. E-mail: jin-chong.tan@eng.ox.ac.uk

^c Diamond Light Source, Diamond House, Harwell Science and Innovation Campus, OX11 0DE Oxfordshire, UK

^d Leverhulme Research Centre of Functional Materials Design, The Materials Innovation Factory, Department of Chemistry, University of Liverpool, L3 3NY Liverpool, UK

† Electronic supplementary information (ESI) available: Experimental section and details on data analysis. CCDC 1892554–1892558. For ESI and crystallographic data in CIF or other electronic format see DOI: 10.1039/c9cc00580c

developments is related to concerns of long-term chemical stability of $[\text{MDABCO}](\text{NH}_4)\text{I}_3$ towards moisture as well as the stress-resistance of the hybrid framework. In particular for device fabrication and durability, the mechanical properties of $[\text{MDABCO}](\text{NH}_4)\text{I}_3$ is of practical importance, *i.e.* the response of $[\text{MDABCO}](\text{NH}_4)\text{I}_3$ to hydrostatic pressure and directionally-induced stress.²⁰ Following the important finding of large spontaneous electric polarization in $[\text{MDABCO}](\text{NH}_4)\text{I}_3$, we probe the mechanical behavior of $[\text{MDABCO}](\text{NH}_4)\text{I}_3$ experimentally. High pressure single crystal diffraction and nanoindentation of single crystals are used to measure the response of $[\text{MDABCO}](\text{NH}_4)\text{I}_3$ towards (uniform) hydrostatic and (non-uniform) directional stress for the first time, deriving the bulk modulus, Young's modulus and hardness of $[\text{MDABCO}](\text{NH}_4)\text{I}_3$.

Single crystals of $[\text{MDABCO}](\text{NH}_4)\text{I}_3$ were synthesized by following the approach from ref. 15, see ESI† for details. Single crystals of $[\text{MDABCO}](\text{NH}_4)\text{I}_3$ grow as rhombohedral plates, with two long and one very short axis. For details of the (high pressure) single crystal diffraction experiments at $p = \text{ambient}$, 0.23, 0.46, 0.72 and 1.28 GPa, see ESI.† In agreement with the previous report,¹⁵ we find $[\text{MDABCO}](\text{NH}_4)\text{I}_3$ crystallizes in the rhombohedral non-centrosymmetric space-group $R3$ solved in the hexagonal setting with $a = 9.8206(5)$ Å, $c = 13.6904(7)$ Å, see Fig. 1a. $[\text{MDABCO}](\text{NH}_4)\text{I}_3$ exhibits the abovementioned perovskite-motif, in which the 3D ReO_3 -type network is formed by $[(\text{NH}_4)\text{I}_3]^{2-}$. Within the 3D network, three hydrogen bonding interactions between $(\text{NH}_4)^+$ and I^- are formed, leading to three long ($d_{\text{long}}(\text{N-I}) = 3.684(10)$ Å) and three short distances ($d_{\text{short}}(\text{N-I}) = 3.642(12)$ Å) within the $(\text{NH}_4)\text{I}_6$ octahedrons, see Fig. S1 (ESI†). $[\text{MDABCO}]^{2+}$ is located within the void of the network, with the C_3 -axis lying along the c -axis of the unit cell and along the body diagonal of the 3D ReO_3 network.

The bonding situation, specifically the absence of strong metal-linker coordination bonds within the ReO_3 network of $[\text{MDABCO}](\text{NH}_4)\text{I}_3$ is unique compared to related HOIPs such as $[(\text{CH}_3)_2\text{NH}_2]\text{Mn}(\text{HCOO})_3$ and is best compared with the metal-free perovskite $[\text{C}_4\text{N}_2\text{H}_{12}][\text{NH}_4]\text{Cl}_3 \cdot \text{H}_2\text{O}$.^{5,19} The bulk modulus K defined through $K = -V(\partial p/\partial V)$ with $V =$ the unit cell volume, and $(\partial p/\partial V)$ the derivative of pressure with respect to volume provides a good comparison for the response of materials to pressure. K is closely related to the strengths and

nature of the chemical bonds within the respective material, and more generally is a measure of the resistivity of the crystal structure against volumetric deformation. For $[\text{MDABCO}](\text{NH}_4)\text{I}_3$, increasing the pressure from $p = \text{ambient}$ to $p = 1.28$ GPa leads to a decrease of unit cell volume from $V_{\text{ambient}} = 1143.47(15)$ Å³ to $V_{1.28\text{GPa}} = 1061.6(5)$ Å³ (Fig. 1b). During high pressure diffraction data analysis, *i.e.* data indexing, data integration and structure solution, no evidence for a phase transition was observed. The bulk modulus for $[\text{MDABCO}](\text{NH}_4)\text{I}_3$ was derived by fitting a 2nd order Birch–Murnaghan equation of state to the measured $P(V)$ data. We obtain 15.19 ± 0.70 GPa, see Fig. 1b and ESI† for details. Despite the absence of a metal center and directional coordination bonds, this bulk modulus is typical for HOIPs such as $[\text{CH}_3\text{NH}_3]\text{PbI}_3$ ($K = 14.8$ GPa),²¹ $[\text{CH}_3\text{NH}_3]\text{PbBr}_3$ ($K = 17.6$ GPa),²² $[\text{CH}_3\text{NH}_3]\text{SnI}_3$ ($K = 12.3$ GPa),²³ $[(\text{CH}_3)_2\text{NH}_2]\text{M}(\text{HCOO})_3$ with $\text{M} = \text{Cu}$, Mn and Fe (K between 24.4 GPa and 27.2 GPa)²⁴ and $[\text{NH}_3\text{NH}_2]\text{Zn}(\text{HCOO})_3$ ($K = 18$ GPa), see Table S2 (ESI†).¹⁰ In HOIPs, the metal center and therewith coordination bond strength typically determines the mechanical response of such materials,^{25–27} and in turn the absence of a metal center in the network of $[\text{MDABCO}](\text{NH}_4)\text{I}_3$ seems to be compensated by hydrogen bonding interactions within the ReO_3 -type network and between $[\text{MDABCO}]^{2+}$ and the network. Comparing bulk moduli of HOIPs to typical oxide ferroelectrics, *e.g.* BaTiO_3 , $\text{Pb}(\text{Zr}_{1-x}\text{Ti}_x)\text{O}_3$ or KNbO_3 with bulk moduli frequently exceeding $K > 100$ GPa, the difference in bonding situation and physical density becomes apparent. In BaTiO_3 , for example, strong ionic interactions between Ba^{2+} and the $[\text{TiO}_3]^{2-}$ network exist, whilst strong covalent interactions dominate in the network itself.²⁸

Structural changes as a function of pressure (*i.e.* bond distances and angles) can also be tracked in the HPSCXRD experiments performed here. We find that volume compression mainly originates from a reduction of nitrogen-iodine bond lengths and distortion of $[(\text{NH}_4)\text{I}_6]$ -octahedrons rather than an increase of octahedral tilting (N-I-N angle), where no clear trend could be observed, see Fig. S2 (ESI†). For instance, the average distance within the $[(\text{NH}_4)\text{I}_6]$ octahedra reduces from $d_{p=\text{ambient}}(\text{N-I}) = 3.663$ Å to $d_{p=1.28\text{GPa}}(\text{N-I}) = 3.59$ Å. In general, HOIPs with X being a monoatomic ion show a large propensity for a decreasing B-X-B angle when put under stress. For instance, in the HOIP $[\text{CH}_3\text{NH}_3]\text{PbI}_3$, the Pb-I-Pb angle decreases from 163.75° to 161.5° when going from ambient pressure to approximately $p = 0.25$ GPa.²⁹ It is worthwhile noting, however, that at ambient pressure $[\text{CH}_3\text{NH}_3]\text{PbI}_3$ crystallizes in the tetragonal space-group $I4/mcm$, in which octahedral tilting is only allowed along one direction. In $[\text{MDABCO}](\text{NH}_4)\text{I}_3$, the octahedrons are much more distorted, showing two different N-I bond lengths as imposed by the rhombohedral symmetry. It therefore seems, that whilst the general bonding energies and physical densities match those of related HOIP materials as reflected in a similar bulk modulus, the bonding situation in $[\text{MDABCO}](\text{NH}_4)\text{I}_3$ is unique as enforced by the molecular nature of the molecular B-site cation that leads to hydrogen bonding interactions between $[\text{NH}_4]^+$ and I^- .

To gain further insight into the mechanical response of $[\text{MDABCO}](\text{NH}_4)\text{I}_3$ to directionally applied stress, we performed

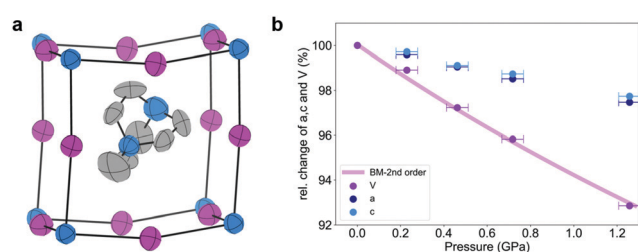


Fig. 1 Schematic of the perovskite structure of $[\text{MDABCO}](\text{NH}_4)\text{I}_3$ (a) with blue = nitrogen, grey = carbon and purple = iodine; hydrogen atoms are not shown for clarity. In (b) the relative change of volume (purple), and the lattice parameters a (dark blue) and c (light blue) are shown as a function of pressure. The plum coloured line corresponds to a 2nd order Birch Murnaghan equation of state with 15.19 ± 0.70 GPa.

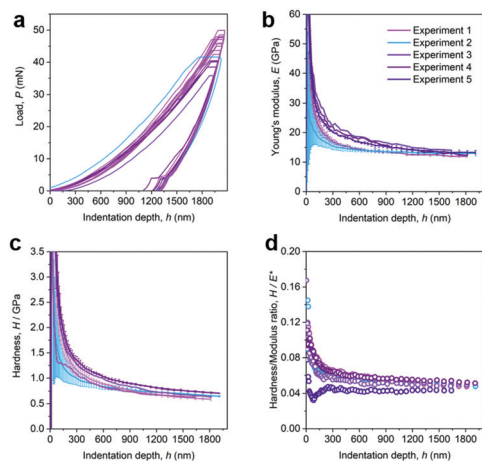


Fig. 2 (a) The force-displacement (P - h) curves of the (111) facet of [MDABCO](NH₄)I₃ crystal measured by nanoindentation, where the P - h curves have been shifted along the horizontal axis for improved comparison of the unloading test segments.³¹ (b) Young's modulus, E , and (c) hardness, H , plotted as a function of the indentation depth, h , obtained from five batches of instrumented nanoindentation experiments. The mean values and standard deviations were acquired based on the data from 500–1900 nm. (d) The ratio of hardness (H) and effective elastic modulus (E^*) presented as a function of h to indicate the plastic deformation relative to the elastic.^{39,40}

nanoindentation experiments along the [111] orientation of the [MDABCO](NH₄)I₃ single crystals. Other directions were not accessible to nanoindentation due to the morphology of [MDABCO](NH₄)I₃ single crystals, see ESI† for details.

For each indentation experiment, a set of force-displacement (P - h) data was recorded, Fig. 2a, from which the Young's modulus and hardness value were derived according to the Oliver-Pharr method.^{30,31} In total, 18 nanoindentation experiments were performed (see Fig. 2a-d and Fig. S3, ESI†), leading to a Young's modulus of $E_{[111]} = 14.7 \pm 1.3$ GPa, and hardness $H = 0.78 \pm 0.06$ GPa (the average values were determined from 500 nm to 1900 nm). Herein, the Poisson's ratio (ν) was taken as 0.2, since the crystal is relatively stiff,³² and the calculation in the Oliver and Pharr method is not dramatically affected by the absolute value of ν .²¹ The indentation modulus for estimating the upper bound of E (set $\nu = 0$) is only slightly lower, see Fig. S3d (ESI†).³¹ Similarly to the bulk modulus, the Young's modulus of [MDABCO](NH₄)I₃ is comparable to the Young's modulus of related HOIPs, e.g. [CH₃NH₃](PbI₃) ($E_{100} = 10.4$ GPa),³³ [CH₃NH₃](PbCl₃) ($E_{100} = 19.8$ GPa), [(NH₂)₂CH](PbI₃) ($E_{100} = 11.8$ GPa),²⁰ and [NH₃NH₂](Zn(HCOO)₃) ($E_{001} = 26.5$ GPa). Previous studies on HOIPs have found that hydrogen bonding interactions between the molecular A-site cation and the negatively charged 3D network to influence the Young's modulus,³⁴ which increases with the number of interactions. In [MDABCO](NH₄)I₃, in principle only the acidic hydrogen atom in [MDABCO]²⁺ is available for reasonably strong hydrogen bonding interactions. The orientation of [MDABCO]²⁺ in the void, i.e. the N-H...I angle and distance of $d(\text{N}_{\text{MDABCO}} \cdots \text{I}) = 3.788$ Å, is unfavorable for the formation of strong hydrogen bonding interactions;³⁵ however, the acidic hydrogen atom is certainly stabilized by three of such interactions, see Fig. S1 (ESI†).

This is in agreement with the observed Young's modulus of [MDABCO](NH₄)I₃ which is at the lower regime of Young's moduli of HOIPs, despite a relatively high packing density resembled by a TF of approx. = 0.93.¹⁵ The observed hardness of the [MDABCO](NH₄)I₃ crystal is approximately 36.8% higher than the [100] facet of [CH₃NH₃](PbI₃).³⁶ This suggests better mechanical durability in resisting permanent plastic deformation, which could induce structural failures of the crystalline material.³⁷ Given the yield strength (σ_y) is normally proportional to hardness,³⁸ [MDABCO](NH₄)I₃ crystals are expected to show a relatively good tolerance of mechanical stress amongst the HOIPs and for retaining the original structure. The topographic imaging of the residual indents using an atomic force microscope (AFM) under the tapping mode, Fig. S3a and b (ESI†), show minor radial cracks and deformation slip steps formation around the residual indents, suggesting plastic flow.

For overviewing our results, the mechanical properties of [MDABCO](NH₄)I₃ are compared to mechanical properties of ceramic ferroelectrics and related HOIPs (see Tables S2 and S3, ESI†). [MDABCO](NH₄)I₃ behaves like a typical dense organic-inorganic framework, despite the different chemical bonding situation, i.e. the absence of directional covalent or coordination bonds in the 3D [(NH₄)I₃]-framework. In fact, similarly as observed in 2002 for [C₄N₂H₁₂](NH₄)Cl₃·H₂O,¹⁹ the 3D framework of [MDABCO](NH₄)I₃ is largely held together by hydrogen bonding interactions. This observation highlights the impact of the relative packing densities and bonding energy per volume unit on the mechanical properties such as the bulk modulus as previously observed for simple oxide materials.⁴¹ In other words, it seems that the Coulomb interactions together with the hydrogen bonding interactions between NH₄⁺ and I⁻ in the 3D [(NH₄)I₃]²⁻ network and the aforementioned hydrogen bonding interactions between [MDABCO]²⁺ and three I⁻ atoms in [MDABCO](NH₄)I₃ lead to a total bond strength per volume unit similar to related dense frameworks with directional covalent or coordination bonds.

In conclusion, we report the first characterization of the mechanical properties of the metal-free ferroelectric [MDABCO](NH₄)I₃. Our findings show that [MDABCO](NH₄)I₃ behaves like a typical dense organic-inorganic perovskite, despite the relatively unusual bonding situation within the 3D framework. Importantly, parallels can be drawn between [MDABCO](NH₄)I₃ and the situation when the large potential of [CH₃NH₃](PbI₃) has initially been discovered.^{42,43} Both materials adopt the perovskite structure motif, can be synthesized by cheap wet-chemistry approaches, and exhibit outstanding properties in their respective areas. The recent progress in preparing flexible photovoltaic devices of [CH₃NH₃](PbI₃) is a further motivation for future research on [MDABCO](NH₄)I₃ and related materials.⁴⁴ In particular, upcoming developments will benefit from the large compositional flexibility of HOIPs, i.e. many different A-B-X permutations are possible when putting [NH₄]⁺ on the B-site and a molecular divalent cation on the A-site.^{1,45,46} Furthermore, our results emphasize the large difference between [MDABCO](NH₄)I₃ and established ferroelectric ceramics, of which the possibility of applying wet-chemistry

techniques for the easy preparation of (flexible) ferroelectric devices seems particularly intriguing. Since oxides typically show a good chemical resistance and great long-time stability, it is important to mention that HOIP ferroelectrics must significantly outperform established ferroelectrics when envisioning the application of HOIPs in non-flexible devices. Therefore, the future challenge related to advancing the application of [MDABCO](NH₄)I₃ seems to be the growth of oriented [MDABCO](NH₄)I₃ films for ferroelectric application for which techniques such as the epitaxial growth or layer-by-layer deposition techniques known from MOFs seem to exhibit the potential in further pushing this area to the next level.⁴⁷ Furthermore, a detailed order-parameter analysis that include the investigation of ferroelastic switching is yet outstanding,⁴⁸ which will certainly provide us with additional insight into the phase transition mechanism on a microscopic level in the near future.¹⁵ Therefore, [MDABCO](NH₄)I₃ as prototypical material of ferroelectric metal-free HOIPs shows all ingredients to start a new era in metal-free ferroelectrics, which will clearly benefit from the large versatility of the perovskite motif, providing a strong platform for rational functional materials design.

The authors would like to thank the Diamond Light Source for beamtime at beamline I19 (MT19080-1). GK would like to thank the FCI for financial support through the Liebig-Fellowship scheme. ME and ZZ contributed equally to this work. SB would like to thank the Hanns-Seidel-Stiftung for financial support funded through a BMBF initiative. MWG thanks the Leverhulme Trust for funding *via* the Leverhulme Research Centre for Functional Materials Design. JCT thanks the ERC Consolidator Grant under the grant agreement 771575 (PROMOFS).

Conflicts of interest

There are no conflicts to declare.

Notes and references

- W. Li, Z. Wang, F. Deschler, S. Gao, R. H. Friend and A. K. Cheetham, *Nat. Rev. Mater.*, 2017, **2**, 16099.
- J. Huang, Y. Yuan, Y. Shao and Y. Yan, *Nat. Rev. Mater.*, 2017, **2**, 17042.
- B. V. Lotsch, *Angew. Chem., Int. Ed.*, 2014, **53**, 635–637.
- J. M. Bermúdez-García, M. Sánchez-Andújar, S. Castro-García, J. López-Beceiro, R. Artiaga and M. A. Señaris-Rodríguez, *Nat. Commun.*, 2017, **8**, 15715.
- P. Jain, V. Ramachandran, R. J. Clark, H. D. Zhou, B. H. Toby, N. S. Dalal, H. W. Kroto and A. K. Cheetham, *J. Am. Chem. Soc.*, 2009, **131**, 13625–13627.
- S. Burger, M. G. Ehrenreich and G. Kieslich, *J. Mater. Chem. A*, 2018, **6**, 21785–21793.
- G. Kieslich, S. Sun and A. K. Cheetham, *Chem. Sci.*, 2014, **5**, 4712–4715.
- K. T. Butler, K. Svane, G. Kieslich, A. K. Cheetham and A. Walsh, *Phys. Rev. B*, 2016, **94**, 180103.
- W. Wei, W. Li, K. T. Butler, G. Feng, C. J. Howard, M. A. Carpenter, P. Lu, A. Walsh and A. K. Cheetham, *Angew. Chem., Int. Ed.*, 2018, **57**, 8932–8936.
- G. Kieslich, A. C. Forse, S. Sun, K. T. Butler, S. Kumagai, Y. Wu, M. R. Warren, A. Walsh, C. P. Grey and A. K. Cheetham, *Chem. Mater.*, 2016, **28**, 312–317.
- J.-H. Lee, N. C. Bristowe, P. D. Bristowe and A. K. Cheetham, *Chem. Commun.*, 2015, **51**, 6434–6437.
- N. L. Evans, P. M. M. Thygesen, H. L. B. Boström, E. M. Reynolds, I. E. Collings, A. E. Phillips and A. L. Goodwin, *J. Am. Chem. Soc.*, 2016, **138**, 9393–9396.
- G. Kieslich and A. L. Goodwin, *Mater. Horiz.*, 2017, **4**, 362–366.
- G. Kieslich, S. Kumagai, A. C. Forse, S. Sun, S. Henke, M. Yamashita, C. P. Grey and A. K. Cheetham, *Chem. Sci.*, 2016, **7**, 5108–5112.
- H.-Y. Ye, Y.-Y. Tang, P.-F. Li, W.-Q. Liao, J.-X. Gao, X.-N. Hua, H. Cai, P.-P. Shi, Y.-M. You and R.-G. Xiong, *Science*, 2018, **361**, 151–155.
- J. Valasek, *Phys. Rev.*, 1921, **17**, 475–481.
- D.-W. Fu, H.-L. Cai, Y. Liu, Q. Ye, W. Zhang, Y. Zhang, X.-Y. Chen, G. Giovannetti, M. Capone, J. Li and R.-G. Xiong, *Science*, 2013, **339**, 425–428.
- G. Shirane, S. Hoshino and K. Suzuki, *Phys. Rev.*, 1950, **80**, 1105–1106.
- C. A. Bremner, M. Simpson and W. T. A. Harrison, *J. Am. Chem. Soc.*, 2002, **124**, 10960–10961.
- S. Sun, F. H. Isikgor, Z. Deng, F. Wei, G. Kieslich, P. D. Bristowe, J. Ouyang and A. K. Cheetham, *ChemSusChem*, 2017, **10**, 3740–3745.
- A. C. Ferreira, A. Létoublon, S. Paofai, S. Raymond, C. Ecolivet, B. Rufflé, S. Cordier, C. Katan, M. I. Saidaminov, A. A. Zhumekenov, O. M. Bakr, J. Even and P. Bourges, *Phys. Rev. Lett.*, 2018, **121**, 085502.
- A. Jaffe, Y. Lin, C. M. Beavers, J. Voss, W. L. Mao and H. I. Karunadasa, *ACS Cent. Sci.*, 2016, **2**, 201–209.
- X. Lü, Y. Wang, C. C. Stoumpos, Q. Hu, X. Guo, H. Chen, L. Yang, J. S. Smith, W. Yang, Y. Zhao, H. Xu, M. G. Kanatzidis and Q. Jia, *Adv. Mater.*, 2016, **28**, 8663–8668.
- I. E. Collings, M. Bykov, E. Bykova, M. Hanfland, S. van Smaalen, L. Dubrovinsky and N. Dubrovinskaya, *CrystEngComm*, 2018, **20**, 3512–3521.
- J.-C. Tan, P. Jain and A. K. Cheetham, *Dalton Trans.*, 2012, **41**, 3949–3952.
- D. Gui, L. Ji, A. Muhammad, W. Li, W. Cai, Y. Li, X. Li, X. Wu and P. Lu, *J. Phys. Chem. Lett.*, 2018, **9**, 751–755.
- L. Xin, Z. Zhang, M. A. Carpenter, M. Zhang, F. Jin, Q. Zhang, X. Wang, W. Tang and X. Lou, *Adv. Funct. Mater.*, 2018, **28**, 1806013.
- S. Saha, T. P. Sinha and A. Mookerjee, *Phys. Rev. B: Condens. Matter Mater. Phys.*, 2000, **62**, 8828–8834.
- M. Szafranski and A. Katrusiak, *J. Phys. Chem. Lett.*, 2017, **8**, 2496–2506.
- W. C. Oliver and G. M. Pharr, *J. Mater. Res.*, 2011, **19**, 3–20.
- J. C. Tan, C. A. Merrill, J. B. Orton and A. K. Cheetham, *Acta Mater.*, 2009, **57**, 3481–3496.
- J. Feng, *APL Mater.*, 2014, **2**, 081801.
- S. Sun, Y. Fang, G. Kieslich, T. J. White and A. K. Cheetham, *J. Mater. Chem. A*, 2015, **3**, 18450–18455.
- W. Li, A. Thirumurugan, P. T. Barton, Z. Lin, S. Henke, H. H. M. Yeung, M. T. Wharmby, E. G. Bithell, C. J. Howard and A. K. Cheetham, *J. Am. Chem. Soc.*, 2014, **136**, 7801–7804.
- T. Steiner, *Angew. Chem., Int. Ed.*, 2002, **41**, 48–76.
- Y. Rakita, S. R. Cohen, N. K. Kedem, G. Hodes and D. Cahen, *MRS Commun.*, 2015, **5**, 623–629.
- Z. Zeng and J.-C. Tan, *ACS Appl. Mater. Interfaces*, 2017, **9**, 39839–39854.
- D. Tabor, *Philos. Mag. A*, 1996, **74**, 1207–1212.
- Y.-T. Cheng and C.-M. Cheng, *Appl. Phys. Lett.*, 1998, **73**, 614–616.
- J. C. Tan, T. D. Bennett and A. K. Cheetham, *Proc. Natl. Acad. Sci. U. S. A.*, 2010, **107**, 9938–9943.
- O. L. Anderson and J. E. Nafe, *J. Geophys. Res.*, 1965, **70**, 3951–3963.
- A. Kojima, K. Teshima, Y. Shirai and T. Miyasaka, *J. Am. Chem. Soc.*, 2009, **131**, 6050–6051.
- M. M. Lee, J. Teuscher, T. Miyasaka, T. N. Murakami and H. J. Snaith, *Science*, 2012, **338**, 643–647.
- F. Di Giacomo, A. Fakharuddin, R. Jose and T. M. Brown, *Energy Environ. Sci.*, 2016, **9**, 3007–3035.
- B. Saporov and D. B. Mitzi, *Chem. Rev.*, 2016, **116**, 4558–4596.
- W.-J. Xu, Z.-Y. Du, W.-X. Zhang and X.-M. Chen, *CrystEngComm*, 2016, **18**, 7915–7928.
- A. Bétard and R. A. Fischer, *Chem. Rev.*, 2012, **112**, 1055–1083.
- W. Li, Z. Zhang, E. Bithell, A. Batsanov, P. Barton, P. Saines, P. Jain, C. Howard, M. Carpenter and A. K. Cheetham, *Acta Mater.*, 2013, **61**, 4928–4938.